

Nanoparticle and Ultrafine Particle Events at the Fresno Supersite

John G. Watson, Judith C. Chow, Kihong Park, and Douglas H. Lowenthal
Desert Research Institute, Reno, NV

Kihong Park
Gwangju Institute of Science and Technology, Gwangju, Korea

ABSTRACT

Continuous measurements of particle size distributions of 3–407 nm were collected from August 2002 to July 2004 at the Fresno Supersite to understand their number concentrations, size distributions, and formation processes. Measurements for fine particulate matter (PM_{2.5}) mass, sulfate (SO₄²⁻), nitrate (NO₃⁻), black carbon (BC), particle-bound polycyclic aromatic hydrocarbons (PAHs), nitrogen oxides (NO_x), carbon monoxide (CO), ozone (O₃), and meteorological data (wind speed, wind direction, temperature [T], relative humidity [RH], and solar radiation) were used to determine the causes of nanoparticle (3–10 nm) and ultrafine (10–100 nm) particle events. These events were found to be divided into four types: (1) 3- to 10-nm morning nucleation; (2) 10- to 30-nm morning traffic; (3) 10- to 30-nm afternoon photochemical; and (4) 50- to 84-nm evening home heating, including residential wood combustion. Intense examples of the first type (>10⁴ number [#]/cm³) were observed on 29 days, nearly always during the summer. The second type of event was observed on more than 73 days and occurred throughout the year. The third type was observed on 36 days, from spring through summer. The fourth type was found on 109 days, all of them during the winter. Although sulfur dioxide (SO₂) emissions in Central California are low, the small residual amounts in gasoline and diesel fuel are apparently sufficient to initiate nucleation events. These were measured in the morning, soon after the shallow surface inversion coupled with layers aloft where nucleation probably was initiated. PM_{2.5} concentrations were poorly correlated with nanoparticle number.

IMPLICATIONS

Nanoparticles and ultrafine particles may cause adverse health effects. Some of these are from locally generated engine and home heating combustion. However, the smallest particles form from photochemical reactions and may be more difficult to control. Nanoparticles and ultrafine particle concentrations are not well-represented by compliance-oriented PM_{2.5} measurements. PM_{2.5} emission reduction strategies might not be sufficient to reduce human exposure to these very small particles.

INTRODUCTION

The presence of nanoparticles (< ~10 nm) in ambient air may adversely affect public health and climate^{1,2} because of their ability to form and grow quickly into ultrafine (~10 to 100 nm) and accumulation (~100 to 1000 nm) modes, then persist for several days. Nanoparticle formation has been observed in a wide variety of environments, including arctic, marine, nonurban continental, and urban areas.^{3–10} Sulfuric acid (H₂SO₄) and water (H₂O) vapors are believed to be the major participants in atmospheric nucleation processes,^{3,11} but the observed production rates are often orders of magnitude higher than can be expected from this binary mechanism.^{3,12,13} Ternary (H₂SO₄)-(NH₃[ammonia])-(H₂O) nucleation, organic vapor nucleation, and ion-induced nucleation mechanisms may explain these observed production rates.³ Binary (H₂SO₄)-(H₂O) nucleation rates might also be enhanced by two or more orders of magnitude when air parcels with large temperature (T) and relative humidity (RH) differences rapidly mix.¹⁴ After freshly nucleated particles are produced, condensation of H₂SO₄, NH₃, and H₂O may contribute to particle growth. Both condensation of organic vapors and heterogeneous reactions may also enhance particle growth rates.^{4,11–13,15,16}

Continuous size distribution measurements in urban areas (e.g., Atlanta, GA, and Pittsburgh, PA) in the Eastern United States show that nanoparticle events correlate with sulfur dioxide (SO₂) concentrations.^{7,10} Woo et al.¹⁰ observed three types of nanoparticle and ultrafine particle events, with characteristic sizes of 3–10, 10–35, and 35–45 nm at the Atlanta Supersite, where a high frequency of events occurred in spring and summer. Abundant nitrogen oxides (NO_x) were found before all the events, during which SO₂ concentrations were elevated. At the Pittsburgh Supersite, Stanier et al.⁷ observed events during all seasons, with the highest frequencies in spring and fall. Satellite site measurements showed that these occurred over a wide area. H₂SO₄ production was associated with UV intensity, consistent with nucleation being initiated by photochemical H₂SO₄ production. In contrast, Watson et al.¹⁷ observed nanoparticle events at the Fresno Supersite during spring and summer that were associated with negligible SO₂ concentrations (i.e., SO₂ concentrations were below the 1 ppbv detection limits of the SO₂ monitor). Fresno's location in Central California is distant from large sulfur emitters, although some SO₂

Table 1. Summary of continuous gas, particle, and meteorological measurements at the Fresno, CA, Supersite.

Observables	Averaging Time	Data Period	Instrument	Model and Manufacturer
N(3–84 nm) (#/cm ³)	5 min	Aug 2002–July 2004 ^a	Nano SMPS	Model SMPS 3936 N25, TSI, Shoreview, MN
N(10–407 nm) (#/cm ³)	5 min	Aug 2002–July 2004 ^b	SMPS	Model SMPS 3936L10, TSI, Shoreview, MN
PM _{2.5} mass (μg/m ³)	1 hr	Dec 2003–July 2004	TEOM	Model TEOM 1400a, Rupprecht and Patashnick, Albany, NY
Sulfate (μg/m ³)	10 min	Dec 2003–July 2004	R&P sulfate analyzer	Model R&P 8400N, Rupprecht and Patashnick, Albany, NY
Nitrate (μg/m ³)	10 min	Dec 2003–June 2003	R&P nitrate analyzer	Model R&P 8400N, Rupprecht and Patashnick, Albany, NY
BC (μg/m ³)	5 min	Dec 2003–June 2004	Seven color aethalometer	Model AE-30, Anderson, Smyrna, GA
Particle-bound PAH (fA)	5 min	Aug 2002–June 2004 ^c	PAH monitor	Model PAS 2000, Eco-Chem Analytics, West Hills, CA
NO _x (ppb)	5 min	Aug 2002–July 2004	Chemiluminescence	Model TEI 42, Thermo Electron Inc., Franklin, MA
CO (ppb)	5 min	Aug 2002–July 2004	IR gas filter	Model DASIBI 3008, Environmental Corp., Glendale, CA
O ₃ (ppb)	5 min	Aug 2002–July 2004	UV absorption	Model API 400, API Inc., San Diego, CA
Wind speed (m/s)	5 min	Aug 2002–July 2004	Wind vane	Model Met One 05305L, Grants Pass, OR
Wind direction (degree N)	5 min	Aug 2002–July 2004	Wind anemometer	Model Met One 05305L, Grants Pass, OR
Temperature (°C)	5 min	Aug 2002–July 2004	Platinum resistance sensor	Model Met One CS500L, Grants Pass, OR
RH (%)	5 min	Aug 2002–July 2004	Capacitance sensor	Model Met One CS, Grants Pass, OR
Solar radiation (W/m ²)	5 min	Aug 2002–July 2004	Pyranometer	Model Li-Cor, Lincoln, NE

Notes: ^aMissing data in September 2003, October 2003, November 2003, and April 2004; the start date is August 25, 2002; ^bMissing data in September 2003, October 2003, November 2003, March 2004, and April 2004; the start date is August 25, 2002; ^cMissing data in January 2004 and February 2004. #/cm³ is the number of particles in each cubic centimeter of sampled air.

originates from residual amounts in gasoline and diesel fuel.

This paper further explores nanoparticle and ultrafine particle events at the Fresno Supersite. Seasonal and diurnal variations of particle number concentrations as a function of size from 3 to 407 nm are examined for the period of August 2002 through July 2004. A method is illustrated that uses other Supersite measurements to evaluate the origins of these events.

EXPERIMENTAL METHODS

The Fresno Supersite (3425 First Street, Fresno, CA) is located ~5.5 km northeast of the downtown Fresno commercial district in California’s San Joaquin Valley (SJV).

The Supersite is in an urban/commercial/residential area with moderate traffic levels and is surrounded by commercial buildings, churches, schools, and residences.¹⁸ Sampling inlets are located on the rooftop of a two-story building on the west side of First Street. In addition to gasoline- and diesel-vehicle exhaust, the site is influenced by home heating, cooking, and regional agricultural activities. Oilfields in the southern SJV, ~180 km south-east of Fresno, no longer burn crude oil for steam generation, which was once the major source of sulfur emissions.¹⁹

Table 1 summarizes the measurements, methods, and sampling periods for the data used here. In addition to the nanoparticle and ultrafine particle size and number

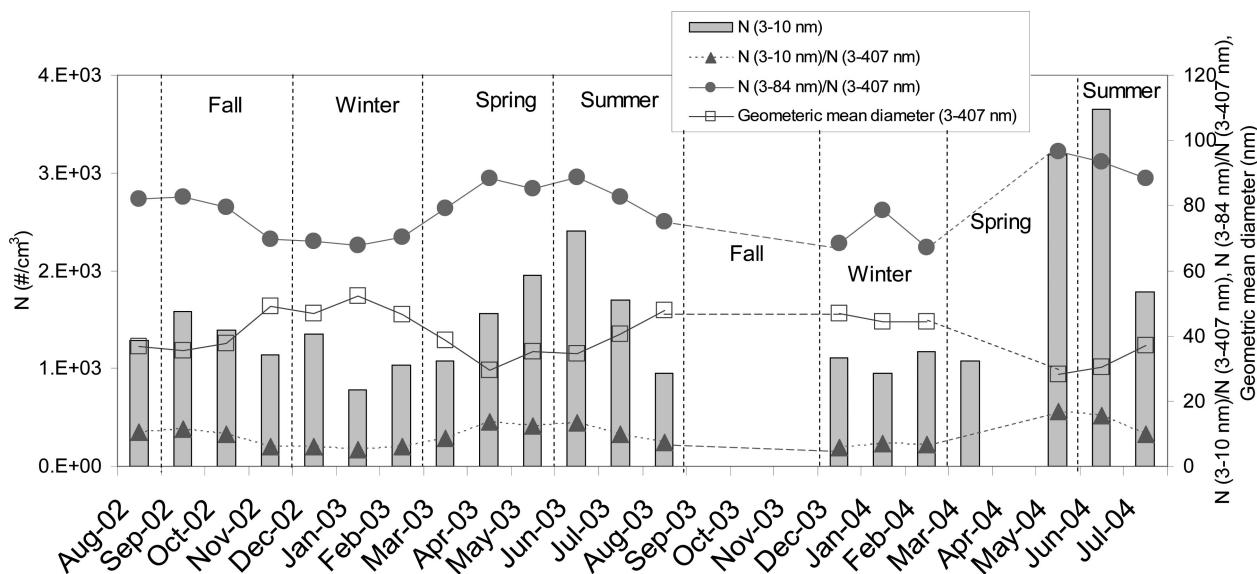


Figure 1. Monthly averages of GMD for N(3–407 nm), N(3–10 nm), the ratio of N(3–10 nm) to N(3–407 nm), and the ratio of N(3–84 nm) to N(3–407 nm). Data from September 2003, October 2003, November 2003, and April 2004 were missing or invalid. PST, hour beginning, is used for all sample durations. Actual time is 1 hr later (Pacific Daylight Time, PDT) from April through October.

measurements, these data include continuous measurements of: (1) fine particulate matter (PM_{2.5}) mass, sulfate (SO₄²⁻), nitrate (NO₃⁻), black carbon (BC), and particle-bound polycyclic aromatic hydrocarbons (PAHs); (2) gaseous NO_x, carbon monoxide (CO), ozone (O₃); and (3) meteorological data (wind speed, wind direction, T, RH, and solar radiation). Operating procedures and results are described elsewhere.^{17,18,20-22}

RESULTS

Seasonal and Diurnal Variations of Particle Number and Size Distribution

Figure 1 shows monthly averages of geometric mean diameter (GMD, from particle number concentration of 3–407 nm), nanoparticle number concentrations [N(3–10 nm)], and the ratios of particle numbers in different size ranges. N(3–10 nm) was higher during summer than winter and peaked in June. A similar pattern was found for the ratios of N(3–10 nm) to N(3–407 nm) and N(3–84 nm) to N(3–407 nm). The GMD varied from 30 to 48 nm during summer, and from 44 to 52 nm during winter.

Lower GMDs during summer are consistent with abundant production of recently formed nanoparticles. This contrasts with colder conditions within a persistent shallow surface layer during winter²⁰ that would favor condensation of vapors onto high concentrations of larger particles. Residential wood combustion (RWC) and other indoor heating emissions are important wintertime sources at Fresno; they are less prevalent during other seasons.^{19,23-25} The maximum 5-min concentrations of N(3–10 nm) and N(3–407 nm) were $\sim 3.3 \times 10^4$ #/cm³ in June 2004 and $\sim 1 \times 10^5$ #/cm³ in December 2003, respectively. Watson et al.¹⁷ reported in June 2003 a maximum 5-min concentration of N(3–10 nm) of 2.4×10^4 #/cm³ for samples acquired August 2002 through July 2003.

Figure 2 compares diurnal variations of particle number concentrations in five size intervals with PM_{2.5} mass, SO₄²⁻, NO₃⁻, BC, PAH, NO_x, and CO. During winter (Figure 2a), particle numbers peaked at $\sim 7:00$ a.m. Pacific Standard Time (PST) for all size ranges. There was a general leveling during late morning and early afternoon. After 3:00 p.m., N(10–30) peaked first, from 6:00 p.m. to

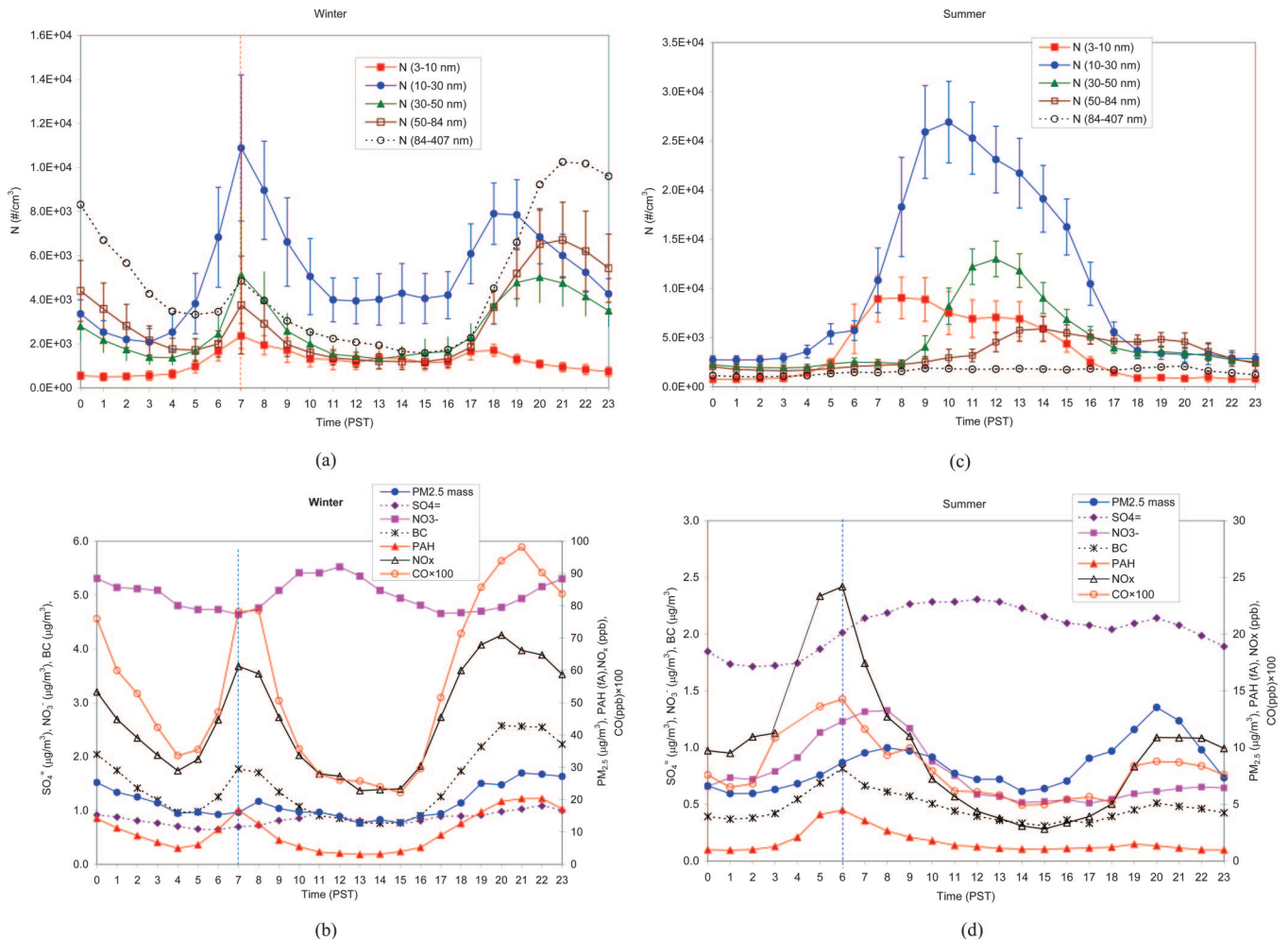


Figure 2. (a) Particle number concentrations in five size intervals averaged by the time of day during winter; (b) PM_{2.5} mass, SO₄²⁻, NO₃⁻, BC, PAHs, NO_x, and CO averaged by the time of day during winter; (c) particle number concentrations in five size intervals averaged by the time of day during summer; and (d) PM_{2.5} mass, SO₄²⁻, NO₃⁻, BC, PAH, NO_x, and CO averaged by the time of day during summer. Particle number counts are divided into the ranges of 3–10 nm, 10–30 nm, 30–50 nm, 50–84 nm, and 84–407 nm. Winter months include December 2002 to February 2003 and December 2003 to February 2004. Summer months include June 2003 to August 2003 and June 2004 to July 2004.

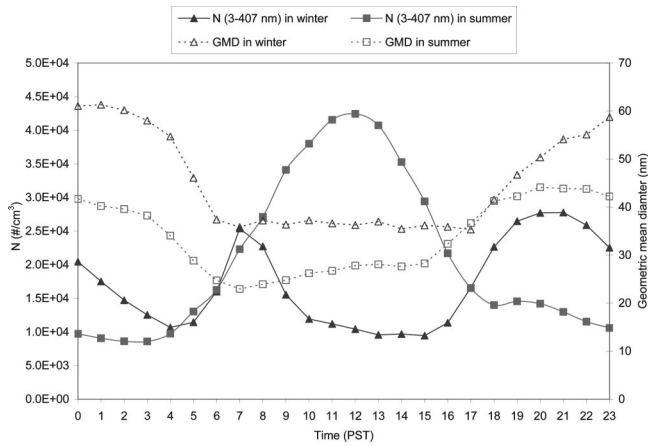


Figure 3. Diurnal variations of GMD and particle number concentration in the size range of 3–407 nm averaged by the time of day in winter (December 2002–February 2003, December 2003–February 2004) and in summer (June 2003–August 2003, June 2004–July 2004).

~7:00 p.m., followed by N(30–50 nm) at 8:00 p.m., as well as N(50–84 nm) and N(84–407 nm) at 9:00 p.m. N(3–10 nm) was a minor fraction of N(3–407) during winter. The morning peaks at 7:00 a.m. coincided with peak concentrations of BC, PAH, NO_x, and CO, consistent with traffic emissions (Figure 2b).

During the evening, the BC and NO_x peaks preceded the PAH and CO peaks, consistent with emissions from lower T combustion sources (such as residential heating) adding to the traffic emissions at night. These peaks followed the expected temporal distributions of emissions in which traffic volume should decrease after the evening rush hour and residential heating emissions increase with the colder nighttime T. It appears that the N(84–407) fraction was largely associated with residential heating.

Increasing NO₃⁻ in the afternoon is consistent with mixing of secondary aerosol formed aloft when the shallow surface layer couples with the valleywide mixed layer.²⁰ This vertical mixing also dilutes the fresh emissions

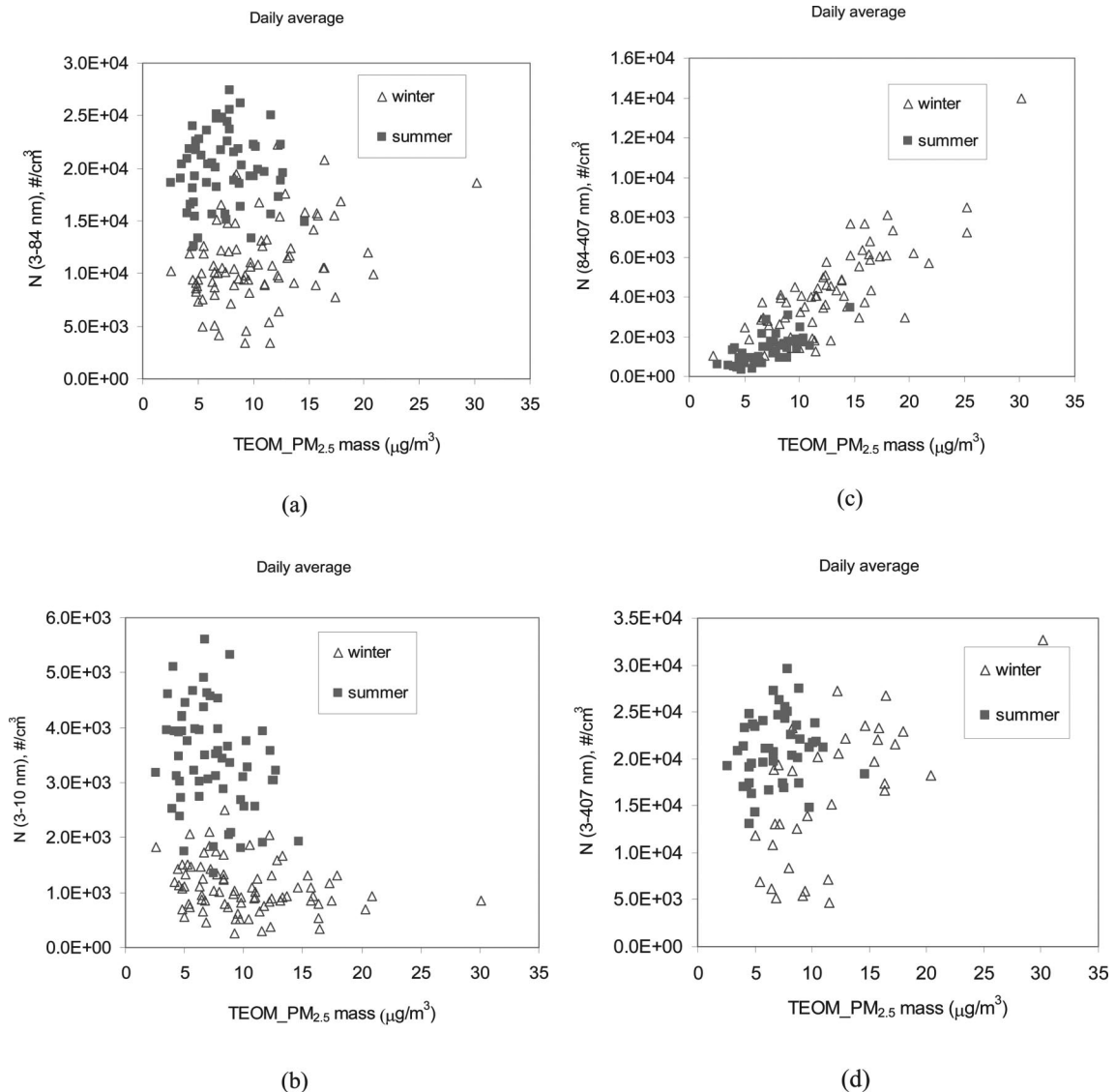


Figure 4. Particle number concentrations in sizes of: (a) 3–10 nm, (b) 3–84 nm, (c) 3–407 nm, and (d) 84–407 nm versus PM_{2.5} mass concentration determined by the Tapered Element Oscillating Microbalance (TEOM, Model 1400a, Rupprecht and Patashnick, Albany, NY).

accumulated under the shallow nighttime inversion. Average SO_4^{2-} was low ($\sim 1 \mu\text{g}/\text{m}^3$) and was fairly constant throughout the day.

During the summer, high values of N(3–10 nm) and N(10–30 nm) occurred, with concentrations peaking at $\sim 8:00$ a.m. and $\sim 10:00$ a.m., respectively, 2–4 hr later than peak concentrations of BC, PAH, NO_x , and CO at $\sim 6:00$ a.m. Evening peaks for BC, PAH, NO_x , and CO were only ~ 20 , ~ 7 , ~ 15 , and $\sim 9\%$ of those found during winter, respectively. SO_4^{2-} levels were twice those during winter ($\sim 2 \mu\text{g}/\text{m}^3$) and reached their maxima during the afternoon. The broad SO_4^{2-} peak from 8:00 a.m. to 3:00 p.m. includes N(3–10 nm) and N(10–30 nm) maxima, consistent with gas-to-particle conversion processes that might accompany nucleation.

Figure 3 contrasts winter and summer GMD and N(3–407 nm). The GMD was always higher during the winter. During the summer, the GMD linearly increased from 7:00 a.m. to 1:00 p.m. at a rate of ~ 0.9 nm/hr. The GMD increase after 3:00 p.m. in summer with decreasing N(3–407 nm) is consistent with particle growth and a tailing off of smaller particle production. During winter, the GMD was fairly constant from 7:00 a.m. to 6:00 p.m. and increased with increasing N(3–407 nm), consistent with fresh sources of primary emissions from residential heating.

Comparisons of Particle Number, $\text{PM}_{2.5}$ Mass, and BC Concentrations

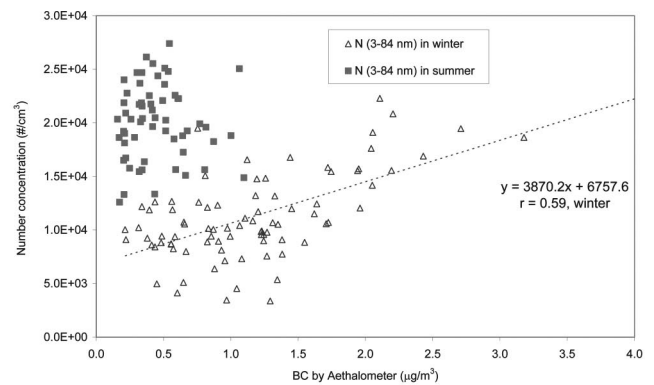
As shown in Figure 4, there is no apparent correlation between particle number and mass concentration except for N(84–407 nm) versus $\text{PM}_{2.5}$. $\text{PM}_{2.5}$ mass is dominated by the accumulation mode and does not represent the mass of nanoparticles and ultrafine particles at Fresno.

N(3–84 nm) is somewhat correlated with BC concentrations during winter, but not during summer, as shown in Figure 5. Even during winter the relationship is poor. This is consistent with roadway particle size measurements taken with thermal denuders^{26–28} in which most of the particles <100 nm were removed at temperatures >250 °C. This would include SO_4^{2-} and many organic compounds, but probably not refractory BC. In contrast, N(84–407 nm) was well-correlated with BC for both seasons, consistent with much of this material being in the larger particle sizes.²⁹

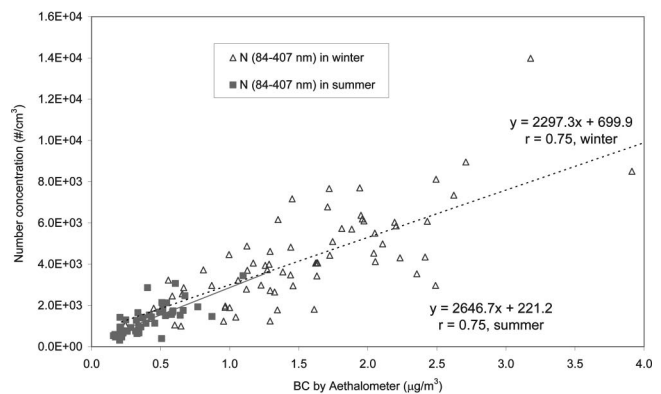
Nanoparticle and Ultrafine Particle Events

Tables 2–5 summarize the days on which different types of events occurred. Meteorological and gas concentration data that support the classification are included. Examples of the temporal and size evolution of these events are depicted in Figure 6.

Days with no events were the most common and appear like that of Figure 6a where no incidences of $N > 10^4$ $\#/\text{cm}^3$ were observed. The 3- to 10-nm nucleation events (Table 2) illustrated in Figure 6b show the familiar “banana-like” growth characteristics observed in the Atlanta, GA¹⁰ and Pittsburgh, PA⁷ Supersites. These events occurred only during late spring and early summer at Fresno. The 3- to 10-nm particles first appear in the early morning $\sim 6:00$ a.m. and peak at 7:00 a.m., followed by a ~ 4 nm/hr particle growth rate. As summarized in Table 2,



(a)



(b)

Figure 5. (a) N(3–84 nm) versus BC concentration; (b) N(84–407 nm) versus BC concentration. The BC concentration was determined by the aethalometer (Model AE-30, Magee Scientific, Berkeley, CA) at a wavelength of 880 nm during winter and summer.

similar characteristics in growth patterns were always observed after the initial nanoparticle burst, although the duration of particle growth differed from day to day. The lowest sizes for these nucleation events are larger than those observed at Atlanta, GA and Pittsburgh, PA, indicating that the nucleation is probably not occurring at ground level. Given the time of the event onset with rising T and dilution of primary pollutants such as BC, it is likely that the nucleation occurred in cleaner air aloft soon after sunrise that was rapidly mixed to the surface.

Figure 7a shows relationships between particle, gas, and meteorological variables associated with the Figure 6b nucleation event. For this Sunday event, there are no increases in BC, NO_x , and CO levels that indicate a traffic event. N(3–10 nm) increased rapidly, by four orders of magnitude over a period of ~ 30 min beginning at $\sim 6:00$ a.m. All of the particle concentrations, including $\text{PM}_{2.5}$ mass, NO_3^- , and BC, were low. Only the SO_4^{2-} concentration increased at the onset of the event, increasing further while the N(3–10 nm) peak decayed 30 min after reaching its maximum of 2.5×10^4 $\#/\text{cm}^3$. SO_4^{2-} remained high until $\sim 3:00$ p.m., consistent with H_2SO_4 vapor contributing to the growth of N(3–10 nm) into larger particles, as postulated at the eastern Supersites. Figure 7b shows that the inception time for the burst of 3–10 nm particles at 6:00 a.m. coincided with the times

Table 2. Summary of 29 morning nucleation events when N(3–10 nm) exceeded 10⁴ #/cm³.

Date	Time	5-min Average				1-hr Average during Event										
		N(3–10 nm) (#/cm ³)		N(3–407 nm) (#/cm ³)		S(3–407) ^c (μm ² /cm ³)	Wind Speed (m/s)	Wind Direction (° North)	T (°C)	RH (%)	Solar Radiation (W/m ²)	BC (μg/m ³)	PAH (IA) Before/ During	NO _x (ppb) Before/ During	CO (ppb) Before/ During	O ₃ (ppb) Before/ During
		Before ^a	During ^b	Before ^a	During ^b											
4/6/03	8–11 a.m.	1.57E+03	1.25E+04	NA	NA	NA	4.7	321	11.9	59.1	651.8	NA	1.50/1.52	26.9/13.9	0.03/0.02	30.8/36.8
5/17/03	7–11 a.m.	2.68E+03	1.24E+04	1.11E+04	2.16E+04	111.4	3.8	309	NA	52.3	295.0	NA	2.21/1.61	20.7/13.1	0.13/0.11	28.8/37.4
5/24/03	6–11 a.m.	2.41E+03	1.38E+04	7.45E+03	2.20E+04	83.1	4.0	315	18.5	61.1	353.2	NA	2.31/1.90	21.1/14.2	0.03/0.02	15.9/24.9
5/25/03	6–10 a.m.	2.34E+03	1.87E+04	5.36E+03	2.80E+04	36.9	2.2	285	15.2	70.2	294.4	NA	1.35/1.59	10.9/5.5	0.03/0.02	20.6/24.4
6/15/03	6–11 a.m.	2.49E+03	1.23E+04	9.61E+03	3.06E+04	101.2	2.7	307	22.8	44.1	595.7	NA	1.78/1.27	13.0/5.7	0.02/0.02	30.0/36.5
6/21/03	6–10 a.m.	4.70E+03	1.30E+04	1.12E+04	2.31E+04	47.6	3.0	321	16.4	61.1	399.5	NA	2.24/1.76	17.6/10.1	0.04/0.04	18.5/27.7
7/11/03	7–10 a.m.	4.66E+03	1.06E+04	1.28E+04	1.89E+04	79.1	2.0	304	24.1	35.8	471.6	NA	6.13/5.44	25.6/22.0	0.04/0.04	11.9/26.3
8/4/03	6–10 a.m.	3.74E+03	1.23E+04	9.69E+03	2.43E+04	64.3	2.4	325	20.8	61.0	432.9	NA	3.52/2.56	14.0/8.1	NA/0.04	9.1/16.9
3/24/04	8–11 a.m.	4.09E+03	1.47E+04	NA	NA	NA	4.2	317	16.9	53.1	712.1	0.33/0.23	1.99/1.98	21.8/11.6	0.05/0.01	25.9/40.2
5/7/04	6 a.m.–1 p.m.	4.71E+03	1.96E+04	1.17E+04	3.13E+04	63.2	4.1	318	16.7	57.2	417.2	0.4/0.3	2.0/1.8	16.8/13.7	0.06/0.06	26.4/32.0
5/8/04	6–11 a.m.	3.88E+03	2.47E+04	8.23E+03	3.53E+04	33.7	4.5	319	16.2	63.9	390.7	0.24/0.17	1.9/1.5	12.8/9.9	0.06/0.06	24.1/30.9
5/9/04	6–10 a.m.	3.51E+03	1.98E+04	9.86E+03	4.05E+04	65.0	4.2	311	16.8	57.7	543.6	0.30/0.19	1.23/0.96	18.3/11.3	0.06/0.09	27.8/34.7
5/15/04	7–11 a.m.	3.49E+03	1.56E+04	1.14E+04	2.79E+04	74.4	2.5	308	20.9	43.8	641.7	0.52/0.42	1.86/1.63	25.9/12.4	0.1/0.1	18.5/29.9
6/2/04	6 a.m.–12 p.m.	4.68E+03	2.03E+04	2.05E+04	4.86E+04	108.8	2.5	326	22.9	44.7	470.7	0.9/0.7	3.2/2.2	27.8/13.9	0.13/0.07	16.6/38.6
6/5/04	6–11 a.m.	5.65E+03	2.25E+04	1.63E+04	6.58E+04	96.3	2.3	337	21.0	41.7	486.0	0.7/0.2	1.9/1.0	25.8/8.5	0.13/0.04	28.0/53.6
6/6/04	6–1 p.m.	4.37E+03	3.35E+04	1.15E+04	4.52E+04	69.8	5.0	330	20.6	51.8	472.8	0.2/0.2	1.0/1.1	5.9/4.5	0.08/0.05	22.4/31.1
6/7/04	6–10 a.m.	6.96E+03	1.77E+04	1.51E+04	2.91E+04	45.3	4.1	310	17.7	54.5	494.5	0.2/0.3	1.5/1.8	13.0/6.0	0.06/0.05	23.0/28.3
6/10/04	6–11 a.m.	3.31E+03	1.37E+04	1.47E+04	2.85E+04	65.5	3.0	308	16.4	63.4	472.9	0.4/0.3	2.8/1.8	24.8/7.9	0.1/0.06	18.1/30.3
6/12/04	6–10 a.m.	4.13E+03	1.21E+04	1.35E+04	2.70E+04	76.3	1.7	320	17.9	51.6	484.4	0.5/0.5	1.5/1.8	25.4/11.6	0.06/0.05	18.5/36.1
6/13/04	6–11 a.m.	3.45E+03	2.35E+04	NA	NA	NA	2.5	328	21.5	49.4	478.0	0.5/0.4	1.2/1.3	10.4/5.6	0.05/0.05	23.7/35.3
6/14/04	6–1 p.m.	6.27E+03	1.87E+04	NA	NA	NA	2.8	319	21.3	55.0	485.8	0.5/0.4	2.7/2.0	17.4/7.1	0.1/0.07	11.8/29.2
6/17/04	6–1 p.m.	4.42E+03	1.53E+04	1.27E+04	2.89E+04	104.5	1.6	281	20.1	62.5	472.1	1.1/0.8	2.8/2.2	17.9/13.3	0.07/0.06	18.1/31.5
6/19/04	6–1 p.m.	3.27E+03	1.23E+04	9.62E+03	2.84E+04	86.5	1.9	319	18.5	66.7	487.8	0.3/0.3	1.3/1.3	10.6/5.0	0.04/0.04	27.2/39.4
6/24/04	6 a.m.–12 p.m.	5.47E+03	1.45E+04	1.34E+04	2.67E+04	83.7	2.0	327	19.4	51.6	491.3	0.5/0.5	2.1/2.0	18.4/10.6	0.21/0.19	16.8/29.5
6/27/04	6 a.m.–12 p.m.	2.31E+03	1.17E+04	5.55E+03	2.07E+04	65.2	2.9	321	19.9	53.6	507.0	0.3/0.2	1.2/1.1	12.3/5.0	NA	19.6/29.4
6/29/04	7–10 a.m.	5.10E+03	1.30E+04	1.42E+04	2.48E+04	95.8	1.8	161	21.6	55.7	664.2	0.7/0.6	3.3/1.9	16.8/13.6	0.09/0.05	21.1/27.7
7/16/04	7–10 a.m.	4.71E+03	1.53E+04	1.30E+04	2.76E+04	67.0	2.3	325	25.0	42.4	472.6	NA	NA	16.4/5.1	0.02/0.02	16.3/33.2
7/18/04	6–10 a.m.	2.82E+03	1.10E+04	8.98E+03	1.79E+04	63.5	2.8	341	24.5	40.3	475.2	NA	NA	8.0/4.8	NA	16.8/31.6
7/20/04	6–11 a.m.	7.04E+03	1.53E+04	1.88E+04	2.96E+04	85.7	3.2	325	23.8	49.9	468.3	NA	NA	18.5/9.3	0.05/0.03	8.7/21.5

^aFive-minute average data before the N(3–10 nm) started to increase; ^b5-min average data at the highest N(3–10 nm); ^c5-min average surface area concentration from 3 to 407 nm.

Table 3. Summary of 36 midday photochemical events when N(10–30 nm) exceeded $2.5 \times 10^4 \text{ \#}/\text{cm}^3$.

Date	Time	5-min Average				1-hr Average during Event										
		N(3–10 nm) (#/cm ³)		N(3–407 nm) (#/cm ³)		S(3–407) ^c (μm ² /cm ³)	Wind Speed (m/s)	Wind Direction (Degree N)	T (°C)	RH (%)	Solar Radiation (W/m ²)	BC (μg/m ³)	PAH (fA)	NO _x (ppb)	CO (ppb)	O ₃ (ppb)
		Before ^a	During ^b	Before ^a	During ^b											
9/23/02	10 a.m.–1 p.m.	5.33E+03	2.94E+04	1.48E+04	4.63E+04	186.1	238.8	153	33.3	26.4	831.0	NA	4.23/2.42	12.4/12.8	0.30/0.33	66.9/108.0
4/10/03	10 a.m.–2 p.m.	7.71E+03	2.86E+04	1.94E+04	3.56E+04	62.9	78.5	299	22.4	45.9	776.0	NA	1.64/2.02	6.2/3.6	0.10/0.04	39.5/58.1
4/12/03	10 a.m.–1 p.m.	1.10E+04	2.68E+04	2.81E+04	3.84E+04	67.9	101.5	293	18.0	55.4	545.1	NA	1.85/1.75	5.7/4.4	0.04/0.04	43.6/47.2
4/24/03	11 a.m.–3 p.m.	6.00E+03	3.22E+04	1.46E+04	4.52E+04	116.0	181.6	158	19.2	44.9	765.0	NA	3.67/3.64	10.7/6.6	0.09/0.05	39.2/46.7
5/15/03	10 a.m.–4 p.m.	1.68E+04	3.02E+04	2.36E+04	6.70E+04	88.7	214.4	239	24.1	37.6	894.0	NA	2.22/1.68	10.4/4.3	0.05/0.03	36.2/53.9
5/23/03	9 p.m.–3 p.m.	6.40E+03	3.12E+04	1.90E+04	5.72E+04	339.9	461.5	177	31.2	34.6	850.0	NA	8.38/2.03	13.8/9.7	0.22/0.20	77.8/100.2
5/26/03	10 a.m.–3 p.m.	3.51E+03	3.16E+04	2.54E+04	5.41E+04	97.4	178.6	311	28.2	34.1	817.0	NA	NA	1.5/0.8	0.03/0.02	40.3/50.4
6/2/03	9 a.m.–2 p.m.	3.01E+03	2.62E+04	1.12E+04	5.44E+04	189.1	328.1	342	32.8	31.3	923.0	NA	4.67/1.41	9.0/3.9	0.20/0.13	64.0/91.4
6/17/03	11 a.m.–4 p.m.	6.33E+03	2.72E+04	1.85E+04	5.53E+04	285.1	252.0	325	34.1	21.6	917.0	NA	3.26/1.78	NA/9.0	NA	NA/38.7
6/18/03	10 p.m.–2 p.m.	1.64E+04	3.30E+04	3.02E+04	5.48E+04	105.1	200.0	325	30.8	23.1	1009.0	NA	1.94/1.50	12.8/5.1	0.13/0.05	42.1/61.7
6/21/03	10 a.m.–4 p.m.	1.86E+04	2.97E+04	2.91E+04	4.87E+04	83.2	150.7	267	23.1	39.3	893.0	NA	1.31/1.22	5.6/4.0	0.05/0.04	38.5/63.5
6/23/03	11 a.m.–4 p.m.	1.46E+04	3.21E+04	2.54E+04	5.75E+04	110.0	169.4	269	27.0	24.6	877.0	NA	2.31/1.46	9.2/2.2	0.09/0.05	43.7/63.7
7/3/03	9 a.m.–4 p.m.	9.42E+03	2.61E+04	2.08E+04	5.18E+04	153.2	224.9	312	33.1	16.2	950.0	NA	4.13/1.31	17.1/6.4	0.11/0.04	45.6/65.7
7/5/03	9 a.m.–4 p.m.	1.26E+04	3.35E+04	2.46E+04	5.22E+04	113.0	168.1	299	31.3	18.8	906.0	NA	2.02/1.13	7.6/2.4	0.05/0.04	55.4/72.5
7/16/03	9 a.m.–1 p.m.	8.31E+03	2.51E+04	2.06E+04	4.04E+04	262.3	344.1	131	31.7	37.5	911.2	NA	5.41/1.93	12.7/6.5	0.23/0.24	58.5/131.9
7/30/03	9 a.m.–2 p.m.	7.19E+03	2.70E+04	1.73E+04	3.97E+04	204.0	226.5	159	34.4	37.7	884.4	NA	5.74/2.73	14.4/9.2	0.19/0.19	68.1/91.7
3/30/04	10 a.m.–1 p.m.	7.52E+03	3.01E+04	NA	NA	NA	NA	327	17.7	59.1	760.5	0.18/0.20	1.39/1.55	8.4/3.6	0.05/0.04	33.9/38.2
5/6/04	11 a.m.–1 p.m.	8.26E+03	3.80E+04	2.20E+04	6.71E+04	190.1	225.4	140	25.8	28.3	718.0	1.1/0.4	3.2/1.4	25.0/12.8	0.25/0.15	40.4/55.9
5/14/04	11 a.m.–2 p.m.	9.11E+03	3.39E+04	2.11E+04	5.60E+04	91.5	198.6	312	29.7	20.3	893.3	0.54/0.48	1.42/1.18	9.0/6.7	0.08/0.09	67.4/75.0
5/24/04	9 a.m.–4 p.m.	1.22E+04	3.01E+04	2.57E+04	4.63E+04	67.9	155.5	27	29.6	38.6	901.7	0.18/0.3	1.17/0.99	6.3/3.5	0.04/0.04	42.5/55.1
6/11/04	10 a.m.–4 p.m.	7.61E+03	3.18E+04	2.04E+04	5.07E+04	147.7	145.5	277	26.4	31.2	898.0	0.6/0.3	2.0/1.2	7.2/2.2	0.05/0.04	50.2/64.5
6/12/04	10 a.m.–3 p.m.	3.89E+03	3.84E+04	1.22E+04	7.56E+04	90.4	250.0	264	29.7	23.3	895.3	0.5/0.3	1.8/1.0	7.6/2.3	0.05/0.04	45.3/74.9
6/13/04	11 a.m.–4 p.m.	2.84E+04	3.54E+04	NA	NA	NA	NA	307	31.5	28.3	895.0	0.2/0.2	0.9/0.9	2.1/2.5	0.04/0.05	58.6/63.0
6/17/04	8 a.m.–3 p.m.	2.04E+04	3.52E+04	3.12E+04	5.50E+04	142.1	174.6	292	25.9	46.4	915.3	0.6/0.4	1.6/1.0	6.9/3.8	0.04/0.04	45.0/62.3
6/20/04	12–5 p.m.	2.61E+04	3.69E+04	5.52E+04	7.26E+04	227.9	245.2	278	30.6	31.5	947.0	0.2/0.2	0.9/0.9	2.1/2.0	0.03/0.01	63.8/68.7
6/21/04	9 a.m.–4 p.m.	1.29E+04	3.39E+04	2.66E+04	5.70E+04	133.4	302.9	271	31.0	31.7	939.3	0.5/0.5	1.3/1.2	5.6/4.4	0.20/0.19	67.6/75.9
6/22/04	11 a.m.–5 p.m.	2.09E+04	3.50E+04	3.89E+04	7.20E+04	226.9	324.4	269	31.8	33.7	972.6	0.9/0.7	2.4/1.2	7.0/4.4	0.03/0.02	70.6/77.5
6/23/04	9 a.m.–4 p.m.	9.68E+03	4.33E+04	2.39E+04	8.53E+04	108.8	369.6	292	29.5	31.5	999.0	0.6/0.5	2.4/1.8	11.0/5.8	0.02/0.02	38.1/54.9
6/28/04	10 a.m.–2 p.m.	5.26E+03	3.09E+04	1.67E+04	5.72E+04	225.2	227.6	238	33.6	23.9	996.0	1.8/0.4	4.0/1.0	28.4/2.8	0.17/0.03	47.6/74.1
7/3/04	10 p.m.–2 p.m.	8.90E+03	3.18E+04	2.13E+04	6.23E+04	211.7	250.4	257	32.5	25.6	1014.4	NA	NA	8.5/2.0	0.06/NA	62.5/63.8
7/7/04	10 a.m.–3 p.m.	9.05E+03	3.38E+04	1.80E+04	5.41E+04	113.7	231.8	242	34.5	23.9	993.2	NA	NA	9.2/3.3	0.03/NA	53.8/71.6
7/13/04	9 a.m.–2 p.m.	1.15E+04	2.67E+04	2.08E+04	4.06E+04	121.0	137.6	247	29.2	26.8	963.3	NA	NA	11.7/6.7	0.02/0.01	45.3/60.0
7/16/04	10 a.m.–4 p.m.	1.97E+04	3.03E+04	3.57E+04	5.32E+04	150.2	233.4	297	32.1	30.1	987.9	NA	NA	9.8/5.5	0.03/0.02	34.6/56.6
7/18/04	8 a.m.–12 p.m.	9.67E+03	3.01E+04	2.16E+04	4.10E+04	72.6	147.4	328	29.2	30.4	780.9	NA	NA	2.6/0.2	NA	44.3/51.8
7/26/04	10 a.m.–1 p.m.	9.26E+03	3.29E+04	2.43E+04	5.22E+04	257.7	311.2	233	35.4	29.6	1015.5	NA	NA	8.7/8.0	0.08/0.06	77.2/105.4
7/28/04	11 a.m.–3 p.m.	8.42E+03	2.89E+04	2.20E+04	4.49E+04	225.9	202.8	260	32.5	26.1	1012.4	NA	NA	NA	NA	NA

^aFive-minute average data before the N(3–10 nm) started to increase; ^b5-min average data at the highest N(3–10 nm); ^c5-min average surface area concentration from 3 to 407 nm.

Table 4. Sixteen examples (one from each month) of 79 morning traffic events when the N(10–30 nm) exceeded $10^4 \text{ \#}/\text{cm}^3$.

Date	Time	5-min Average										1-hr Average during Event									
		N(3–10 nm) (#/cm ³)		N(3–407 nm) (#/cm ³)		S(3–407) ^c (μm ² /cm ³)		Wind Speed (m/s)	Wind Direction (Degree N)	T (°C)	RH (%)	Solar Radiation (W/m ²)	BC (μg/m ³)	PAH (fA)	NO _x (ppb)	CO (ppb)	O ₃ (ppb)				
		Before ^a	During ^b	Before ^a	During ^b	Before ^a	During ^b											Before/	During	Before/	During
9/9/02	6–7 a.m.	8.38E+03	1.94E+04	2.08E+04	5.20E+04	253.4	511.0	0.8	159	15.2	66.1	24.0	NA	13.41/34.91	43.8/103.5	0.72/1.50	4.7/4.9				
10/21/02	6–8 a.m.	9.29E+03	2.18E+04	2.13E+04	3.94E+04	237.0	332.7	1.3	72	10.7	86.7	2.2	NA	6.40/24.58	21.5/81.0	0.45/1.46	1.95/6.9				
11/4/02	6–9 a.m.	9.92E+03	2.71E+04	2.31E+04	5.64E+04	393.3	511.2	0.6	97	7.2	76.4	93.5	NA	14.25/37.96	51.0/107.8	0.86/1.69	3.9/4.6				
12/18/02	7–9 a.m.	8.15E+03	3.84E+04	2.40E+04	7.61E+04	437.1	834.7	1.0	16	1.5	93.9	22.0	NA	26.53/51.86	84.1/226.8	1.33/2.48	3.23/3.58				
1/16/03	6–10 a.m.	2.48E+03	3.54E+04	1.36E+04	6.49E+04	400.0	657.2	0.9	21	3.5	93.5	4.3	NA	23.65/45.90	89.9/272.0	1.04/3.75	2.5/3.0				
2/6/03	6–8 a.m.	9.76E+03	3.76E+04	2.08E+04	6.94E+04	226.9	487.1	1.0	133	2.1	87.6	14.8	NA	14.01/59.49	44.2/137.0	0.66/1.73	2.7/3.0				
3/6/03	5–9 a.m.	9.36E+03	3.30E+04	1.82E+04	5.61E+04	294.8	435.9	0.9	118	7.8	82.2	122.9	NA	11.36/33.71	29.9/104.4	0.35/1.30	3.9/3.9				
4/22/03	5–9 a.m.	4.41E+03	2.01E+04	NA	NA	NA	NA	0.9	209	8.7	88.3	156.9	NA	2.51/14.01	39.4/47.2	0.33/0.47	4.89/7.4				
6/17/03	5–8 a.m.	7.46E+03	3.97E+04	1.68E+04	5.96E+04	223.0	316.6	1.3	280	23.8	50.3	181.4	NA	3.39/16.7	NA/66.0	0.08/0.7	NA				
8/2/03	5–9 a.m.	2.88E+03	1.87E+04	9.12E+03	2.88E+04	121.2	195.0	2.1	293	24.3	59.2	322.2	NA	1.79/2.59	9.4/20.1	0.03/0.06	11.2/10.8				
12/26/03	7–9 a.m.	6.04E+03	2.74E+04	1.06E+04	6.52E+04	799.7	1055.2	1.0	282	4.4	89.3	14.1	2.5/3.8	26.3/33.2	37.2/67.6	0.17/0.43	4.7/7.1				
1/9/04	7–10 a.m.	9.08E+03	2.55E+04	1.81E+04	4.71E+04	145.3	304.4	1.4	91	10.9	62.2	22.7	0.8/1.8	NA	64.1/133.3	0.70/2.01	2.7/3.7				
2/2/04	5–10 a.m.	4.60E+03	1.46E+04	7.65E+03	2.92E+04	104.6	275.5	2.9	136	9.7	62.7	55.1	0.3/1.2	NA	33.4/42.8	0.38/0.41	8.1/8.7				
3/3/04	5–10 a.m.	3.17E+03	3.71E+04	NA	NA	NA	NA	0.9	137	5.3	92.3	9.1	0.86/1.68	7.2/17.4	21.3/45.3	0.26/0.44	5.9/5.2				
5/14/04	5–8 a.m.	6.28E+03	3.52E+04	1.96E+04	5.94E+04	181.2	316.3	1.0	36	14.3	62.9	55.0	1.67/3.05	10.22/18.05	23.9/62.0	0.25/0.86	4.7/8.9				
7/26/04	5–8 a.m.	4.05E+03	1.33E+04	1.46E+04	2.85E+04	258.2	312.5	1.4	115	23.6	63.2	224.1	NA	NA	48.2/68.0	0.74/1.04	2.6/5.3				

^aFive-minute average data before the N(3–10 nm) started to increase; ^b5-min average data at the highest N(3–10 nm); ^c5-min average surface area concentration from 3 to 407 nm.

Table 5. Eight examples (at least one from each winter month) of 109 evening residential heating events when N(50–84 nm) exceeded $10^4 \text{ \#}/\text{cm}^3$.

Date	Time	5-min Average										1-hr Average during Event									
		N(3–10 nm) (#/cm ³)		N(3–407 nm) (#/cm ³)		S(3–407) ^c (μm ² /cm ³)		Wind Speed (m/s)	Wind Direction (Degree N)	T (°C)	RH (%)	Solar Radiation (W/m ²)	BC (μg/m ³)	PAH (fA)	NO _x (ppb)	CO (ppb)	O ₃ (ppb)				
		Before ^a	During ^b	Before ^a	During ^b	Before ^a	During ^b											Before/	During	Before/	During
11/18/02	7 p.m.–12 a.m.	8.39E+03	3.37E+04	2.91E+04	9.63E+04	754.1	3189.4	1.1	149	10.0	90.9	0.0	NA	16.96/86.58	106.3/283.6	1.45/3.96	3.8/5.1				
12/24/02	6 p.m.–12 a.m.	7.84E+03	3.55E+04	1.18E+04	5.12E+04	886.9	3534.9	1.7	331	4.6	89.6	0.0	NA	22.86/128.90	53.2/228.0	0.70/3.30	4.93/9.12				
1/1/03	4 p.m.–12 a.m.	1.45E+03	2.60E+04	7.10E+03	7.48E+04	181.5	2327.9	1.4	301	8.4	83.7	0.0	NA	2.35/55.99	48.0/296.8	0.73/4.80	8.17/6.6				
2/8/03	8 p.m.–12 a.m.	1.14E+04	2.92E+04	4.01E+04	8.38E+04	989.0	2735.0	1.5	40	5.9	68.5	0.0	NA	39.13/90	51.4/271.6	0.68/4.3	7.27/4				
3/1/03	8 p.m.–12 a.m.	4.91E+03	1.15E+04	2.02E+04	3.98E+04	369.0	799.4	1.3	238	9.7	79.3	0.0	NA	9.9/32.9	NA	NA	NA				
12/26/03	8 p.m.–12 a.m.	1.34E+04	3.98E+04	4.73E+04	1.03E+05	1169.5	3060.3	0.8	83	5.1	73.3	0.0	5.2/12.2	38.9/87.9	100.0/180.0	1.40/2.60	5.7/5.1				
1/9/04	9 p.m.–12 a.m.	7.11E+03	1.30E+04	2.95E+04	4.05E+04	593.2	965.7	0.9	110	12.4	66.2	0.0	2.8/4.0	NA	137.7/183.7	1.79/2.40	3.6/3.8				
2/1/04	7 p.m.–12 a.m.	5.39E+03	1.32E+04	2.14E+04	3.93E+04	493.1	1153.4	0.5	120	11.2	61.8	0.0	1.4/3.5	NA	44.4/83.7	0.63/1.47	9.4/4.7				

^aFive-minute average data before the N(3–10 nm) started to increase; ^b5-min average data at the highest N(3–10 nm); ^c5-min average surface area concentration from 3 to 407 nm.

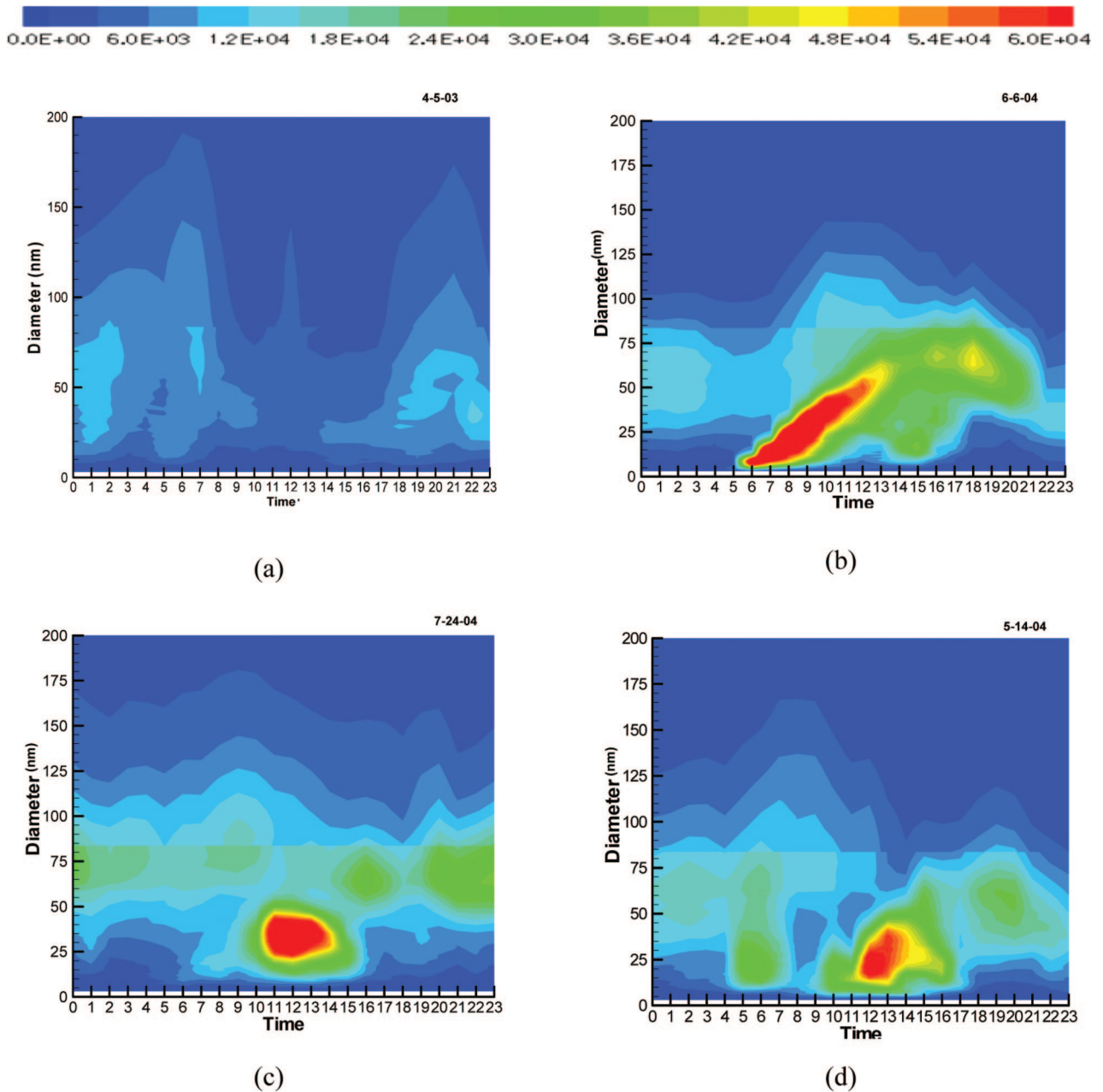


Figure 6. Diurnal variations of particle size distribution with diameter on the y-axis, time of day on the x-axis, and particle concentration ($dN/d\log D_p$) by shading contour for: (a) no event; (b) 3–10 nm nucleation event (Sunday, June 6, 2004); (c) 10–30 nm photochemical event (Saturday, July 24, 2004); (d) 10–30 nm traffic and photochemical events (Friday, May 14, 2004); (e) 3–10 nm nucleation and 10–30 nm photochemical events (Monday, June 14, 2004); (f) 10–30 nm traffic and 50–84 nm residential heating events (Friday, February 6, 2004); and (g) 50–84 nm residential heating event (Sunday, February 1, 2004). The discontinuity at ~ 80 nm is due to slight differences in the responses of the nano-SMPS and standard SMPS.

for increasing O_3 , T, and solar radiation, and for decreasing RH, consistent with vertical mixing and the presence of photochemically produced hydroxyl (OH) radicals that would oxidize available SO_2 to SO_3 . For weekday events (Table 2), the N(3–10 nm) peak does not coincide with morning BC, PAH, NO_x , and CO peaks. Although continuous NH_3 was not measured with these experiments, NH_3 is abundant in the SJV during summer.³⁰ Using a zero dimensional model, Gaydos et al.⁵ found that nucleation rates of $10 \text{ \#/cm}^3\text{-sec}$ were achieved with NH_3 concentrations as low as 10 ppt and H_2SO_4 levels as low as 2.4 ppt.

Although SO_4^{2-} levels are much lower in Fresno than in the Eastern United States, and there is enough NH_3 to completely neutralize H_2SO_4 , the values are higher than 10 ppt. The $(H_2SO_4)\text{-(}NH_3\text{)-(}H_2O\text{)}$ mechanism probably dominates these nucleation events.

The onset of the episode also corresponded to coupling between the morning surface layer and the valleywide mixed layer, as seen by the increase in T and decrease in RH that accompany the rapid increase in N(3–10 nm) in Figure 7b. The surface layer is often cooler and has higher RH than the layer aloft, and the mixing

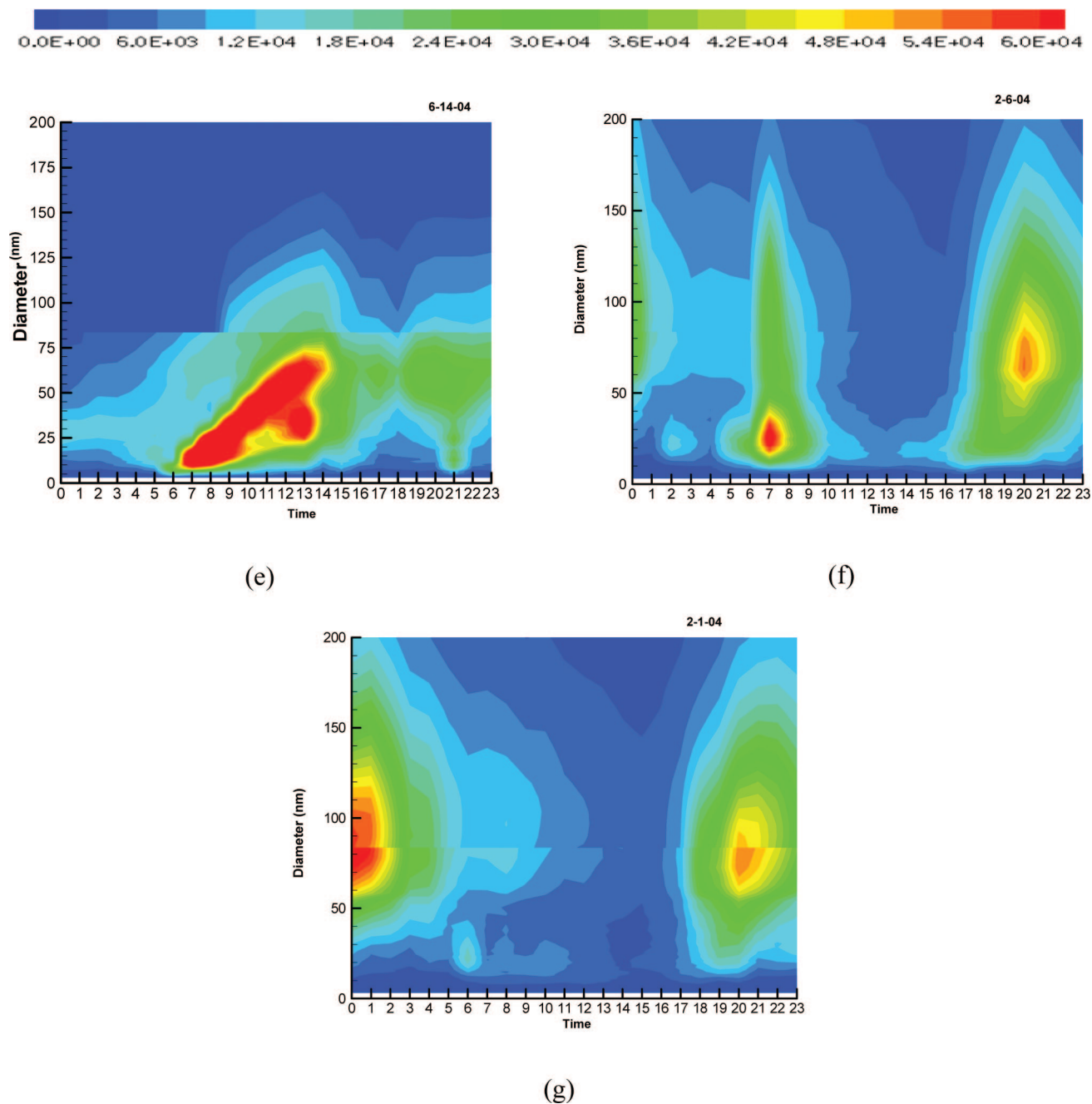


Figure 6. Cont.

mechanism proposed by Nilsson and Kulmala¹⁴ merits further exploration in a future experiment that includes more detailed summertime upper-air measurements.

Figure 7a shows a small secondary nanoparticle event occurring around 2:00–4:00 p.m. The evolution of size distributions for this event is examined in Figure 8. Nanoparticles with a mode diameter of ~ 6 nm appear between 5:00 a.m. and 6:00 a.m., with most of the particles in the ultrafine mode peaking at ~ 60 nm. The onset of the nanoparticle burst occurred at 6:00 a.m. with an 8-nm peak, which quickly grew in number and size through 7:00–8:00 a.m. Particle numbers and sizes in the ~ 50 - to 200-nm region increased slowly during the morning hours. Near noon, nanoparticles almost disappeared with

a single ultrafine mode diameter of ~ 50 nm. They appeared again at $\sim 2:00$ p.m. with a mode of ~ 18 nm, much higher than the morning mode. This afternoon mode lasted until 3:00 p.m., but was depleted by 4:00 p.m. The appearance of nanoparticles in the afternoon is believed to be associated with photochemical reactions and condensation on smaller particles in a deeper well-mixed layer.

Figure 6c represents an afternoon 10- to 30-nm photochemical event. These events (Table 3) typically occurred over a longer time period, spring through fall, than the morning nucleation events. They appear more as midday “blobs” than as “banana-shaped” morning nucleation events. Particle sizes are larger than those of

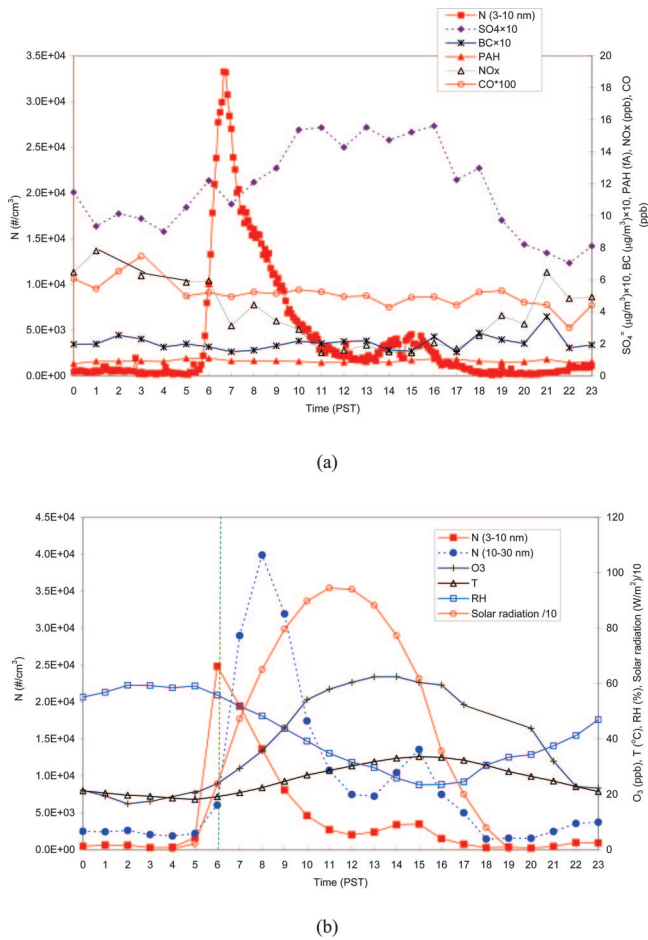


Figure 7. Diurnal variations of: (a) $N(3-10 \text{ nm})$; SO_4^{2-} , BC ($\mu\text{g}/\text{m}^3$), PAH (fA), NO_x (ppb), and CO (ppb); and (b) $N(3-10 \text{ nm})$; $N(10-30 \text{ nm})$; O_3 (ppb), T ($^\circ\text{C}$), RH (%), and solar radiation (W/m^2) corresponding to the 3–10 nm nucleation event on Sunday, June 6, 2004.

nucleation events, but smaller than those from primary emissions. Figure 6d shows a midday 10- to 30-nm photochemical event that occurred after a moderate 10- to 30-nm morning traffic event. In Figure 9, ancillary measurements show the clear peaks in BC, PAH, NO_x , and CO from 5:00 to 7:00 a.m. that would be expected from the Friday morning rush hour. By 11:00 a.m., the primary particles decreased, whereas $N(3-10 \text{ nm})$, $N(10-30 \text{ nm})$, and O_3 increased. $N(10-30 \text{ nm})$ tapered off with O_3 and solar radiation, consistent with a common process affecting them both. Watson et al.¹⁷ identified this as a more aged nucleation event. This may correspond with secondary organic aerosol (SOA) formation, possibly on small H_2SO_4 nuclei, as photochemical processes oxidize lighter volatile organic compounds to heavier semivolatile organic compounds that can condense on pre-existing particles. The lack of correspondence with other measurements at midday rules out primary emitters for these midday surges.

Morning nucleation and afternoon photochemical events often occurred together, as illustrated in Figure 6e. As shown in Tables 2 and 3, similar relationships between particle number concentration and BC, PAH, NO_x , CO, O_3 , and solar radiation, illustrated in Figures 7 and 9, were found repeatedly.

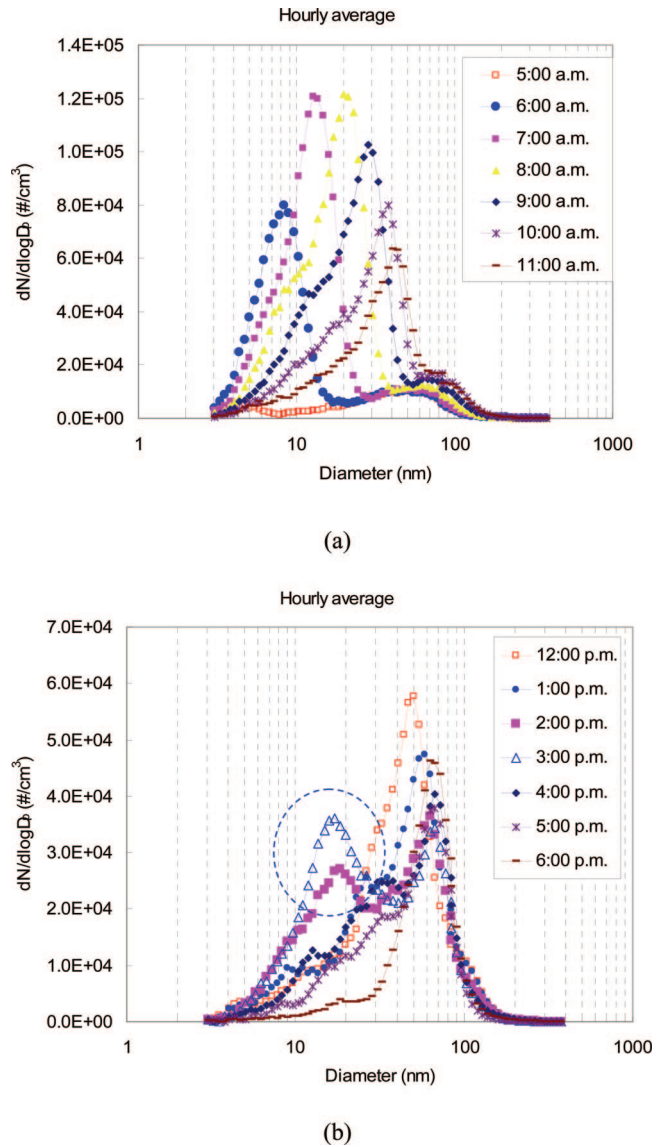
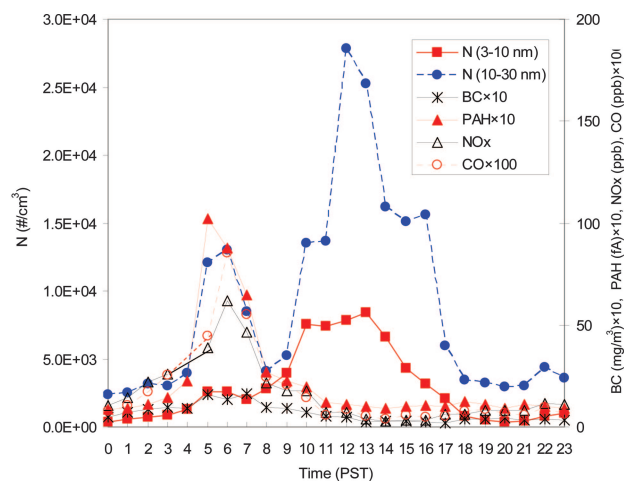
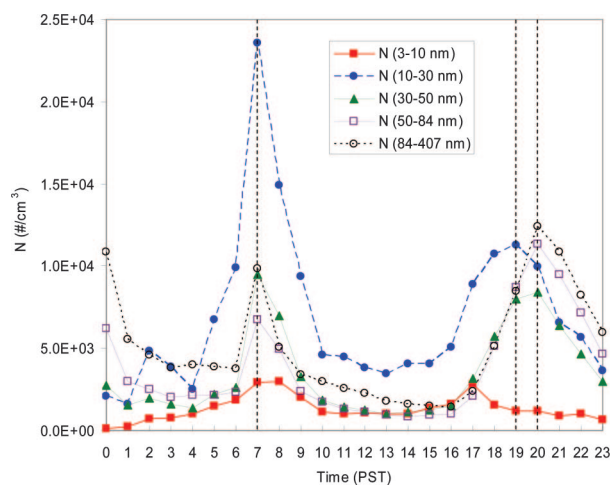


Figure 8. Temporal variations of hourly averages of size distributions with $dN/d\log D_p$ on the y-axis and D_p on the x-axis from 5:00 a.m. to 6:00 p.m. for the 3–10 nm nucleation event on Sunday, June 6, 2004.

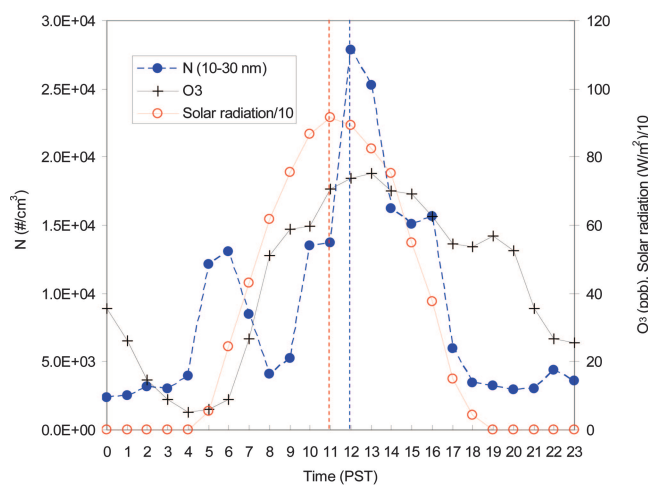
Figure 6f is an example of morning traffic and evening residential heating events. These often occurred together during winter months (Tables 4 and 5), but the residential heating events were not observed during non-winter periods. Morning traffic events were observed throughout the year. Figure 10 shows the relationships between different size fractions and other Fresno measurements corresponding to Figure 6f. High particle number concentrations were observed around 7:00 a.m., lasting only 2 hr before disappearing as the mixed layer developed. In the evening, the particle number concentrations increased from 5:00 p.m. and peaked around 8:00 p.m. with a mean diameter of $\sim 63 \text{ nm}$. Correspondence of the BC, NO_x , and CO with $N(10-30 \text{ nm})$ in the morning is a clear indicator of the traffic contribution. In the evening, the $N(50-84 \text{ nm})$ peak lagged the $N(10-30 \text{ nm})$ peak. $N(50-84 \text{ nm})$ also corresponds to the BC, PAH, and



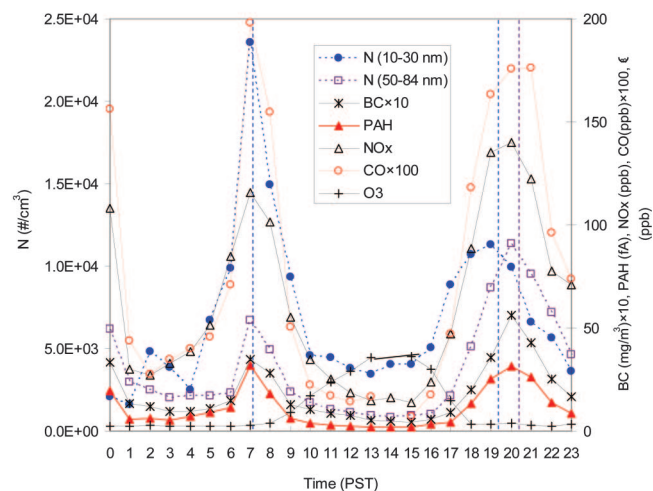
(a)



(a)



(b)



(b)

Figure 9. Diurnal variations of hourly averages of: (a) N(3–10 nm; #/cm³), N(10–30 nm; #/cm³), BC (μg/m³), PAH (fA), NO_x (ppb), and CO (ppb); and (b) N(3–10 nm; #/cm³), O₃ (ppb), and solar radiation (W/m²) for the combined 10–30 nm traffic and photochemical events on Friday, May 14, 2004.

Figure 10. Diurnal variations of hourly averages of (a) N(3–10 nm; #/cm³), N(10–30 nm; #/cm³), N(30–50 nm; #/cm³), N(50–84 nm; #/cm³), and N(84–407 nm; #/cm³); and (b) N(10–30 nm; #/cm³), N(50–84 nm; #/cm³), BC (μg/m³), PAH (fA), NO_x (ppb), CO (ppb), and O₃ (ppb) for the 10–30 nm traffic and 50–84 nm residential heating events on Friday, February 6, 2004.

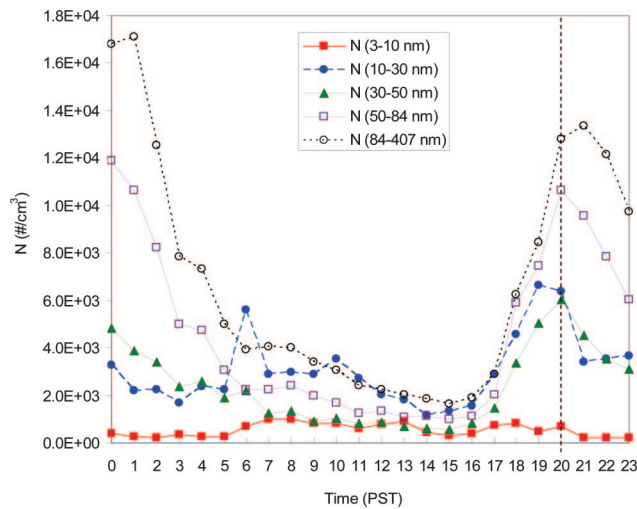
CO peaks better than the NO_x peak, which is closer in time to the N(10–30 nm) peak.

In contrast, Figure 6g presents a similar wintertime Sunday event when morning and evening traffic volumes were lower. Associated Supersite data are shown in Figure 11; N(10–30 nm) was much lower than N(50–84 nm) in the evening compared with that shown in Figure 10. Surface areas for the morning nucleation events were much lower than those for the morning traffic and evening heating events, as shown in Tables 2–5. This is consistent with previous Fresno measurements¹⁷ showing that nanoparticle concentrations and the ratio of nanoparticle to total particle concentration were inversely proportional to particle surface area. This is also consistent with condensable vapors depositing on the surfaces of existing particles rather than nucleating. A relatively low particle surface area is a prerequisite for nucleation. During the 482 days

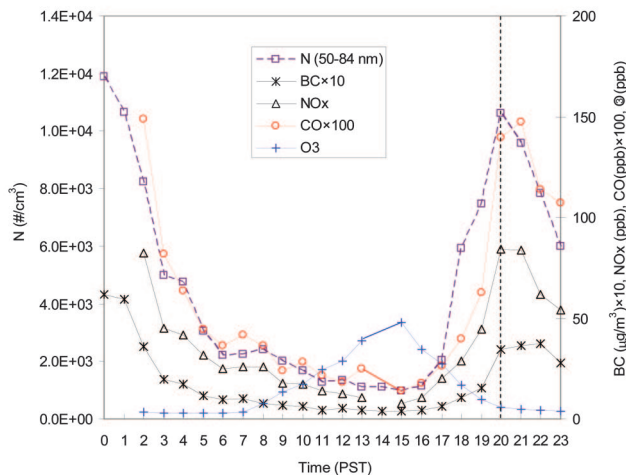
with valid data reported here, 3- to 10-nm morning nucleation events with concentrations greater than 10⁴ #/cm³ were observed on 29 days, mostly during the summer. The 10- to 30-nm morning traffic events with concentrations greater than 10⁴ #/cm³ were observed on 73 days, with the highest frequency during the winter. The 10- to 30-nm afternoon photochemical events with concentrations greater than 2.5 × 10⁴ #/cm³ occurred on 36 days, with the highest frequency during summer. The 50- to 84-nm evening residential heating events with concentrations greater than 10⁴ #/cm³ were observed on 109 days during winter.

CONCLUSIONS

Particle size distributions measured from August 2002 through July 2004 at the Fresno Supersite showed that



(a)



(b)

Figure 11. Diurnal variations of hourly averages of (a) $N(3-10\text{ nm})$, $N(10-30\text{ nm})$, $N(30-50\text{ nm})$, $N(50-84\text{ nm})$, $N(84-407\text{ nm})$; and (b) $N(50-84\text{ nm})$, BC ($\mu\text{g}/\text{m}^3$), NO_x (ppb), CO (ppb), and O_3 (ppb) for the 50–84 nm residential heating event on Sunday, February 1, 2004. PAH data were not available for this event.

nanoparticle concentrations were higher in summer than winter, mainly because of higher production by nucleation and photochemical reaction events. Distinct diurnal variations for particle size and number between summer and winter were observed with high-number concentrations during the early morning and evening periods in winter, and around noontime in summer. Low correlations between $\text{PM}_{2.5}$ mass and particle number concentrations of nanoparticles and ultrafine particles indicate that $\text{PM}_{2.5}$ mass measurements do not represent concentrations of particles $<100\text{ nm}$ in diameter.

Nanoparticle and ultrafine particle events at Fresno can be divided into four classes: (1) 3- to 10-nm morning nucleation, (2) 10- to 30-nm morning traffic, (3) 10- to 30-nm afternoon photochemical, and (4) 50- to 84-nm evening residential heating, including wood combustion.

Ternary (H_2SO_4)-(NH_3)-(H_2O) nucleation aloft with rapid mixing to the surface caused by breakup of the shallow surface inversion might account for the nucleation rates and sizes in the 3- to 10-nm morning nucleation event. The 10- to 30-nm afternoon photochemical effect probably could result from semivolatile organic compounds condensing on a H_2SO_4 core. The other two events are derive from primary emissions from the indicated sources. Analysis of continuous and highly time-resolved measurements with the nanoparticle and ultrafine particle size distributions allows the different formation mechanisms to be distinguished from one another.

ACKNOWLEDGMENTS

The Fresno Supersite is a cooperative effort between the California Air Resources Board (CARB) and the Desert Research Institute (DRI). Sponsorship is provided by the U.S. Environmental Protection Agency through the Cooperative Institute for Atmospheric Sciences and Terrestrial Applications (CIASTA) of the National Oceanic and Atmospheric Administration. The authors thank Peter Ouchida and Scott Scheller of the CARB and Dr. Susanne Hering of Aerosol Dynamics, Inc., for their efforts in maintaining the monitoring instruments. Dr. John Bowen of DRI assisted in field coordination and data processing of Supersite measurements. Jo Gerrard and Tim Richard of DRI assisted in assembling and editing the manuscript.

REFERENCES

- Biswas, P.; Wu, C.Y. 2005 Critical Review: Nanoparticles and the Environment; *J. Air & Waste Manage. Assoc.* **2005**, *55*, 708-746.
- Chow, J.C.; Watson, J.G.; Savage, N.; Solomon, J.; Cheng, Y.S.; McMurry, P.H.; Biswas, P.; Wu, C.Y. Critical Review Discussion: Nanoparticles and the Environment; *J. Air & Waste Manage. Assoc.* **2005**, *55*, 1411-1417.
- Kulmala, M.; Vehkamäki, H.; Petaja, T.; Dal Maso, M.; Lauri, A.; Kerminen, V.M.; Birmili, W.; McMurry, P.H. Formation and Growth Rates of Ultrafine Atmospheric Particles: A Review of Observations; *J. Aerosol. Sci.* **2004**, *35*, 143-176.
- Kulmala, M.; Kerminen, V.M.; Anttila, T.; Laaksonen, A.; O'Dowd, C.D. Organic Aerosol Formation Via Sulphate Cluster Activation; *J. Geophys. Res.* **2004**, *109(D4)*, D04205, doi:10.1029/2003JD003961.
- Gaydos, T.M.; Stanier, C.O.; Pandis, S.N. Modeling of in Situ Ultrafine Atmospheric Particle Formation in the Eastern United States; *J. Geophys. Res.* **2005**, *110(D7)*, D07S12, doi:10.1029/2004JD004683.
- McMurry, P.H.; Woo, K.S.; Weber, R.; Chen, D.R.; Pui, D.Y.H. Size Distributions of 3–10 nm Atmospheric Particles: Implications for Nucleation Mechanisms; *Philos. Trans. R. Soc. London, Ser A* **2000**, *358*, 2625-2642.
- Stanier, C.O.; Khlystov, A.Y.; Pandis, S.N. Nucleation Events during the Pittsburgh Air Quality Study: Description and Relation to Key Meteorological, Gas Phase, and Aerosol Parameters; *Aerosol Sci. Technol.* **2004**, *38(Suppl. 1)*, 253-264. ISI:000221762100021.
- Stanier, C.O.; Khlystov, A.Y.; Pandis, S.N. Ambient Aerosol Size Distributions and Number Concentrations Measured during the Pittsburgh Air Quality Study (PAQS); *Atmos. Environ.* **2004**, *38*, 3275-3284.
- Tolocka, M.P.; Lake, D.A.; Johnston, M.V.; Wexler, A.S. Size-Resolved Fine and Ultrafine Particle Composition in Baltimore, Maryland; *J. Geophys. Res.* **2005**, *110(D7)*, D07S04, doi:10.1029/2004JD004573.
- Woo, K.S.; Chen, D.R.; Pui, D.Y.H.; McMurry, P.H. Measurement of Atlanta Aerosol Size Distributions: Observations of Ultrafine Particle Events; *Aerosol Sci. Technol.* **2001**, *34*, 75-87.
- Eisele, F.L.; McMurry, P.H. Recent Progress in Understanding Particle Nucleation and Growth; *Philos. Trans. R. Soc. London Ser. B* **1997**, *352*, 191-200.
- Weber, R.J.; Marti, J.J.; McMurry, P.H.; Eisele, F.L.; Tanner, D.J.; Jefferson, A. Measurements of New Particle Formation and Ultrafine Particle Growth Rates at a Clean Continental Site; *J. Geophys. Res.* **1997**, *102*, 4375-4386.
- Weber, R.J.; McMurry, P.H.; Mauldin, R.L., III; Tanner, D.J.; Eisele, F.L.; Clarke, A.D.; Kapustin, V.N. New Particle Formation in the Remote Troposphere: A Comparison of Observations at Various Sites; *Geophys. Res. Lett.* **1999**, *26*, 307-310.

14. Nilsson, E.D.; Kulmala, M. The Potential for Atmospheric Mixing Processes to Enhance the Binary Nucleation Rate; *J. Geophys. Res.* **1998**, *103*, 1381-1389.
15. O'Dowd, C.D.; Jimenez, J.L.; Bahreini, R.; Flagan, R.C.; Seinfeld, J.H.; Hameri, K.; Pirjola, L.; Kulmala, M.; Jennings, S.G.; Hoffmann, T. Marine Aerosol Formation from Biogenic Iodine Emissions; *Nature* **2002**, *417*, 632-636.
16. Zhang, K.M.; Wexler, A.S. A Hypothesis for Growth of Fresh Atmospheric Nuclei; *J. Geophys. Res.* **2002**, *107(D21)*, AAC 15-1-AAC 15-6, doi:10.1029/2002JD002180.
17. Watson, J.G.; Chow, J.C.; Lowenthal, D.H.; Kreisberg, N.; Hering, S.V.; Stolzenburg, M.R. Variations of Nanoparticle Concentrations at the Fresno Supersite; *Sci. Total Environ.* **2006**, in press.
18. Watson, J.G.; Chow, J.C.; Bowen, J.L.; Lowenthal, D.H.; Hering, S.; Ouchida, P.; Oslund, W. Air Quality Measurements from the Fresno Supersite; *J. Air & Waste Manage. Assoc.* **2000**, *50*, 1321-1334.
19. Chow, J.C.; Watson, J.G.; Lowenthal, D.H.; Solomon, P.A.; Magliano, K.L.; Ziman, S.D.; Richards, L.W. PM₁₀ Source Apportionment in California's San Joaquin Valley; *Atmos. Environ.* **1992**, *26A*, 3335-3354.
20. Watson, J.G.; Chow, J.C. A Wintertime PM_{2.5} Episode at the Fresno, CA, Supersite; *Atmos. Environ.* **2002a**, *36*, 465-475.
21. Watson, J.G.; Chow, J.C. Comparison and Evaluation of in-Situ and Filter Carbon Measurements at the Fresno Supersite; *J. Geophys. Res.* **2002b**, *107(D21)*, ICC 3-1-ICC 3-15, doi: 10.1029/2001JD000573.
22. Watson, J.G.; Chow, J.C.; Lowenthal, D.H.; Stolzenburg, M.R.; Kreisberg, N.M.; Hering, S.V. Particle Size Relationships at the Fresno Supersite; *J. Air & Waste Manage. Assoc.* **2002**, *52*, 822-827.
23. Poore, M.W. Levoglucosan in PM_{2.5} at the Fresno Supersite; *J. Air & Waste Manage. Assoc.* **2002**, *52*, 3-4.
24. Schauer, J.J.; Cass, G.R. Source Apportionment of Wintertime Gas-Phase and Particle-Phase Air Pollutants Using Organic Compounds as Tracers; *Environ. Sci. Technol.* **2000**, *34*, 1821-1832.
25. Rinehart, L.R.; Fujita, E.M.; Chow, J.C.; Magliano, K.; Zielinska, B. Spatial Distribution of PM_{2.5} Associated Organic Compounds in Central California; *Atmos. Environ.* **2006**, *46*, 290-303.
26. Hasegawa, S.; Hirabayashi, M.; Kobayashi, S.; Moriguchi, Y.; Kondo, Y.; Tanabe, K.; Wakamatsu, S. Size Distribution and Characterization of Ultrafine Particles in Roadside Atmosphere; *J. Environ. Sci. Health, Part A-Toxics/Haz. Subst. & Env. Eng.* **2004**, *39*, 2671-2690.
27. Kittelson, D.B.; Watts, W.F.; Johnson, J.P.; Remerowki, M.L.; Ische, E.E.; Oberdörster, G.; Gelein, R.A.; Elder, A.; Hopke, P.K.; Kim, E.; Zhao, W.; Zhou, L.; Jeong, C.H. On-Road Exposure to Highway Aerosols. 1. Aerosol and Gas Measurements; *Inhal. Toxicol.* **2004**, *16(Suppl. 1)*, 31-39.
28. Kuhn, T.; Krudysz, M.; Zhu, Y.F.; Fine, P.M.; Hinds, W.C.; Froines, J.; Sioutas, C. Volatility of Indoor and Outdoor Ultrafine Particulate Matter near a Freeway; *J. Aerosol. Sci.* **2005**, *36*, 291-302.
29. Kittelson, D.B. Engines and Nanoparticles: A Review; *J. Aerosol. Sci.* **1998**, *29*, 575-588.
30. Chow, J.C.; Watson, J.G.; Lowenthal, D.H.; Egami, R.T.; Solomon, P.A.; Thuillier, R.H.; Magliano, K.L.; Ranzieri, A.J. Spatial and Temporal Variations of Particulate Precursor Gases and Photochemical Reaction Products during SJVAQS/AUSPEX Ozone Episodes; *Atmos. Environ.* **1998**, *32*, 2835-2844.

About the Authors

John G. Watson and Judith C. Chow are research professors, and Douglas H. Lowenthal is an associate research professor, at the Desert Research Institute (DRI). Kihong Park, formerly an assistant research professor at DRI, is currently an assistant professor at Gwangju Institute of Science and Technology. Address correspondence to: Judith C. Chow, Division of Atmospheric Sciences, Desert Research Institute, 2215 Raggio Parkway, Reno, NV, 89512; phone: +1-775-674-7050; fax: +1-775-674-7009; e-mail: judyc@dri.edu.